

Electronic Supplementary Information (ESI) for

Symmetry and Spacing Controls in Periodic Covalent Functionalization of Graphite Surfaces Templated by Self-Assembled Molecular Networks

Shingo Hashimoto,^a Hiromasa Kaneko,^a Steven De Feyter,^b Yoshito Tobe,^{c,d} and Kazukuni Tahara^{*a}

^a Department of Applied Chemistry, School of Science and Technology, Meiji University, 1-1-1 Higashimita, Tama-ku, Kawasaki, Kanagawa, 214-8571, Japan.

^b Division of Molecular Imaging and Photonics, Department of Chemistry, KU Leuven, Celestijnenlaan 200 F, 3001 Leuven, Belgium.

^c Department of Applied Chemistry, National Yang Ming Chiao Tung University, 1001 Ta Hsueh Road, Hsinchu 30030, Taiwan.

^d The Institute of Scientific and Industrial Research, Osaka University, Ibaraki, Osaka 567-0047, Japan.

*Correspondence author: tahara@meiji.ac.jp

This file includes:

1. Supramolecular Chirality of BisDBA SAMNs	S2
2. Cyclic Voltammograms, Additional Raman Spectrum and Chronoamperograms.....	S3
4. Non-zoomed 2D-FFT Images	S6
5. Fidelity Analysis	S7
6. Additional Fidelity Analysis.....	S9
7. Additional STM Image of Functionalized Surface with bisDBA-C14 Template	S10
8. Molecular Mechanics (MM) Simulations	S10
9. Additional Data for Positional Analysis of Grafted Aryls in Pores	S12
10. Covalent Functionalization around the Domain Boundary	S13
11. Additional STM Images of SAMN Formed by BisDBA-C12.....	S14
12. Reference.....	S17

1. Supramolecular Chirality of BisDBA SAMNs

In the STM observations of SAMNs of **bisDBA-C10** and **-C12**, there are two enantiomorph domains of the Kagomé and porous C structures (Figure S1).

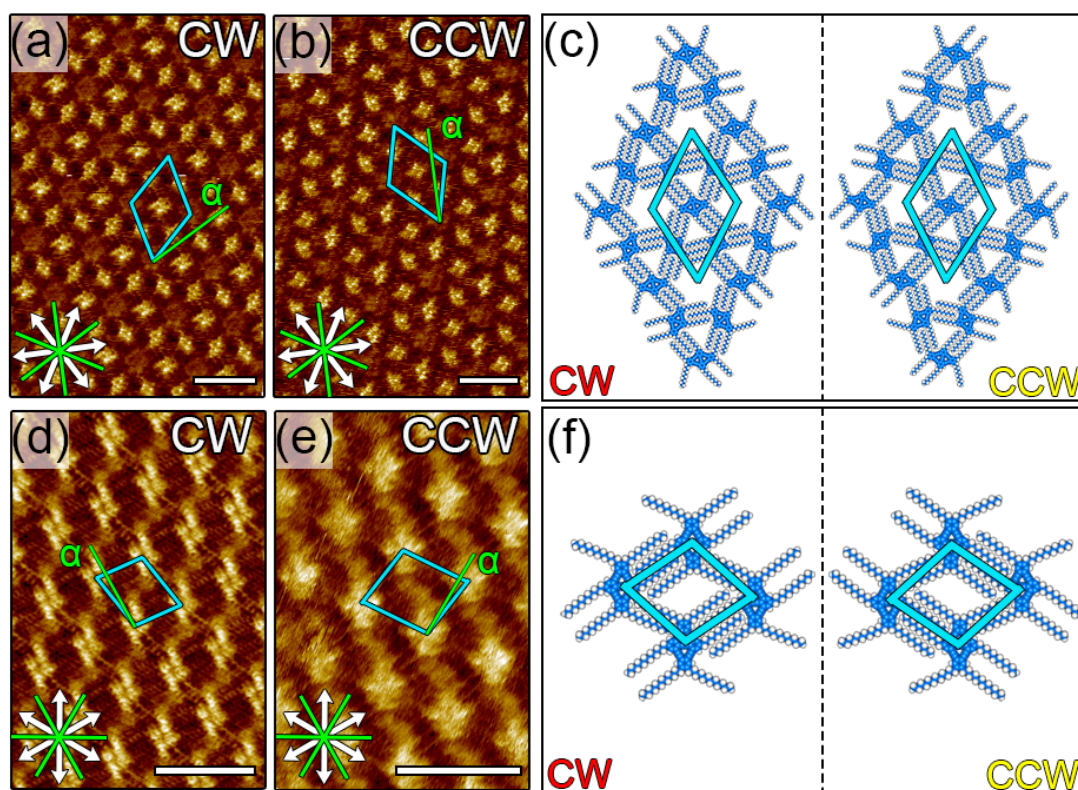


Figure S1. (a, b, d, e) High-resolution STM images of the CW (a, d) and CCW (b, e) structures of the Kagomé (a, b) and Porous C (d, e) structures formed by **bisDBA-C10** and **-C12**, respectively. White arrows in the lower left corner and green lines indicate the main symmetry axes of graphite substrate underneath and the in-plane directions normal to those, respectively. Turquoise rhombi in the images are unit cells. Angle α is between one of the unit cell vectors and the closest normal to the graphite main symmetry axes. Unit cell parameters and angle α are summarized in Table 1 in the main text. Scale bars: 5 nm. Tunneling parameters: (a, b) $V_{\text{bias}} = -0.92$ V, $I_{\text{set}} = 67$ pA; (d) $V_{\text{bias}} = -1.06$ V, $I_{\text{set}} = 130$ pA; (e) $V_{\text{bias}} = -0.41$ V, $I_{\text{set}} = 250$ pA. (c, f) MM optimized models of the Kagomé (c) and Porous C (f) structures formed by **bisDBA-C10** and **C12**, respectively. In these models, the orientations of the molecular models do not correspond to those of the STM images (a, b, d, e). Carbon atoms: blue; hydrogen atoms: white. (c, f) Left and right models are the CW and CCW structures, respectively.

2. Cyclic Voltammograms, Additional Raman Spectrum and Chronoamperograms

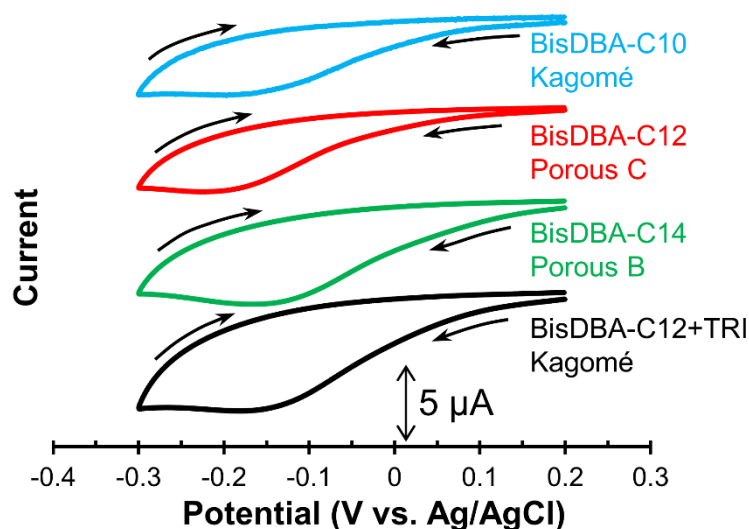


Figure S2. Cyclic voltammograms (a single cycle from +0.20 to -0.30 V, vs Ag/AgCl, 0.1 V/s) during the electrochemical grafting of graphite using TMeOD in the presence of a solution of **bisDBA** in TCB as an interfacial layer. Raman spectra of the functionalized surfaces by CV are shown in Figure S4. Light blue: the surface with the Kagomé structure of **bisDBA-C10**; red: the surface with the Porous C structure of **bisDBA-C12**; green: the surface with the Porous B structure of **bisDBA-C14**; black: the surface with the Kagomé structure of **bisDBA-C12+TRI**.

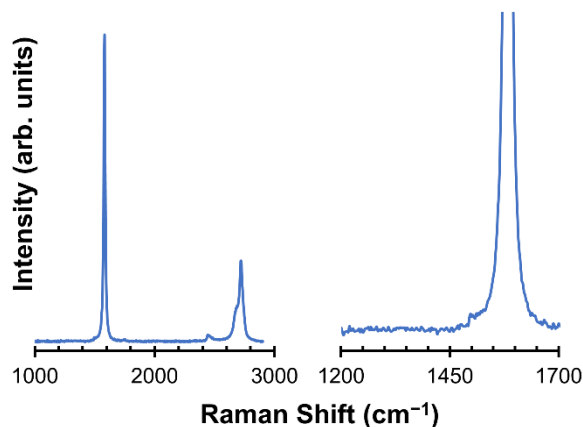


Figure S3. Raman spectrum of the pristine HOPG surface. No D peak was observed.

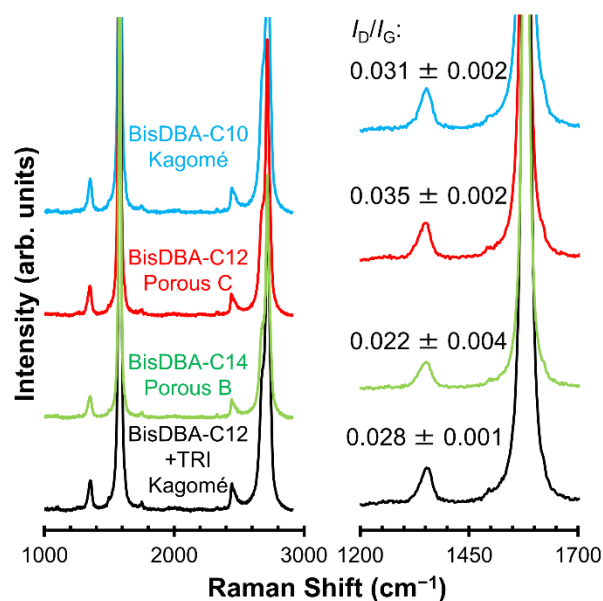


Figure S4. Raman spectra of the functionalized graphite surfaces using CV. Black numbers in the right images are mean I_D/I_G ratios. The excitation laser wavelength is 532 nm. Blue: Kagomé structure formed by **bisDBA-C10**; red: Porous C structure formed by **bisDBA-C12**; green: Porous B structure formed by **bisDBA-C14**; black: Kagomé structure formed by **bisDBA-C12+TRI**. The concentration of 3,4,5-trimethoxyaniline was set to be 1.0 mM.

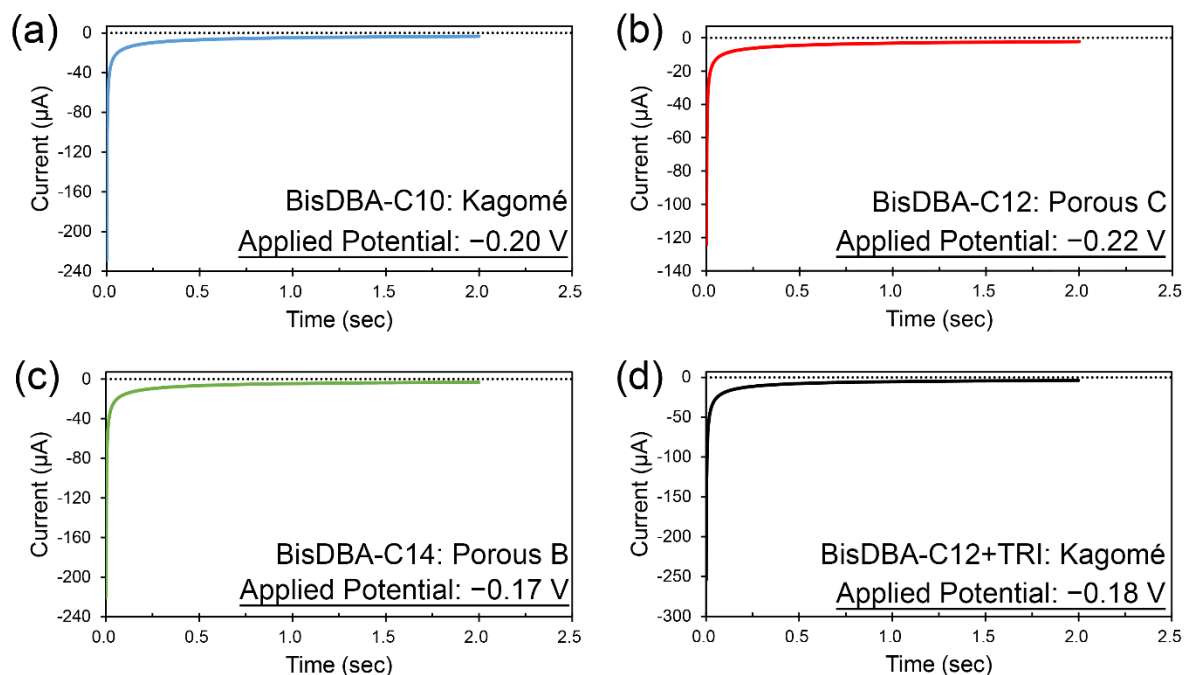


Figure S5. Chronoamperograms during the electrochemical grafting of graphite in the presence of a solution of (a) **bisDBA-C10**, (b) **-C12**, (c) **-C14**, or (d) **bisDBA-C12+TRI** in TCB as an interfacial layer. The concentration of 3,4,5-trimethoxyaniline was set to be 0.5 mM. Applied potentials for 2 sec. are (a) -0.20 V, (b) -0.22 V, (c) -0.17 V, or (d) -0.18 V (vs. Ag/AgCl).

3. Height Analyses of STM Images of Functionalized Surfaces

To investigate the apparent heights of the grafted aryls and **bisDBA** π -cores, we conducted apparent height analyses using the STM images of the functionalized surfaces after the template-guided grafting. The representative height profile of the functionalized surface is shown in Figure S6. The apparent height of the **bisDBA** π -cores is approximately 50–80 pm, while that of the aryls is over 100 pm.

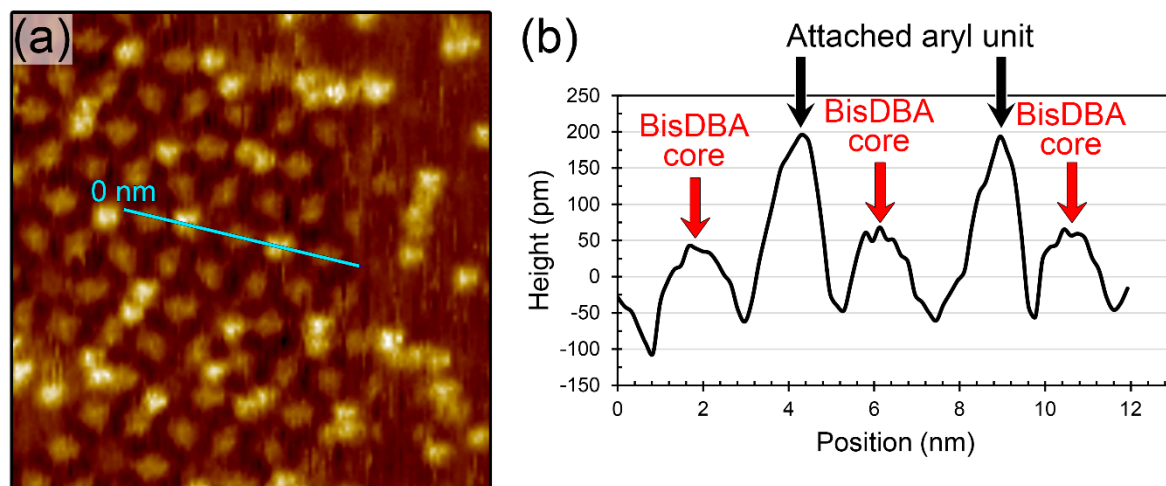


Figure S6. (a) STM image of the functionalized HOPG surface using the Kagomé structure formed by **bisDBA-C10** as the template. (b) Height profile along the turquoise line in (a). Red and black arrows indicate the positions of the **bisDBA** π -core and grafted aryl units, respectively.

4. Non-Zoomed 2D-FFT Images

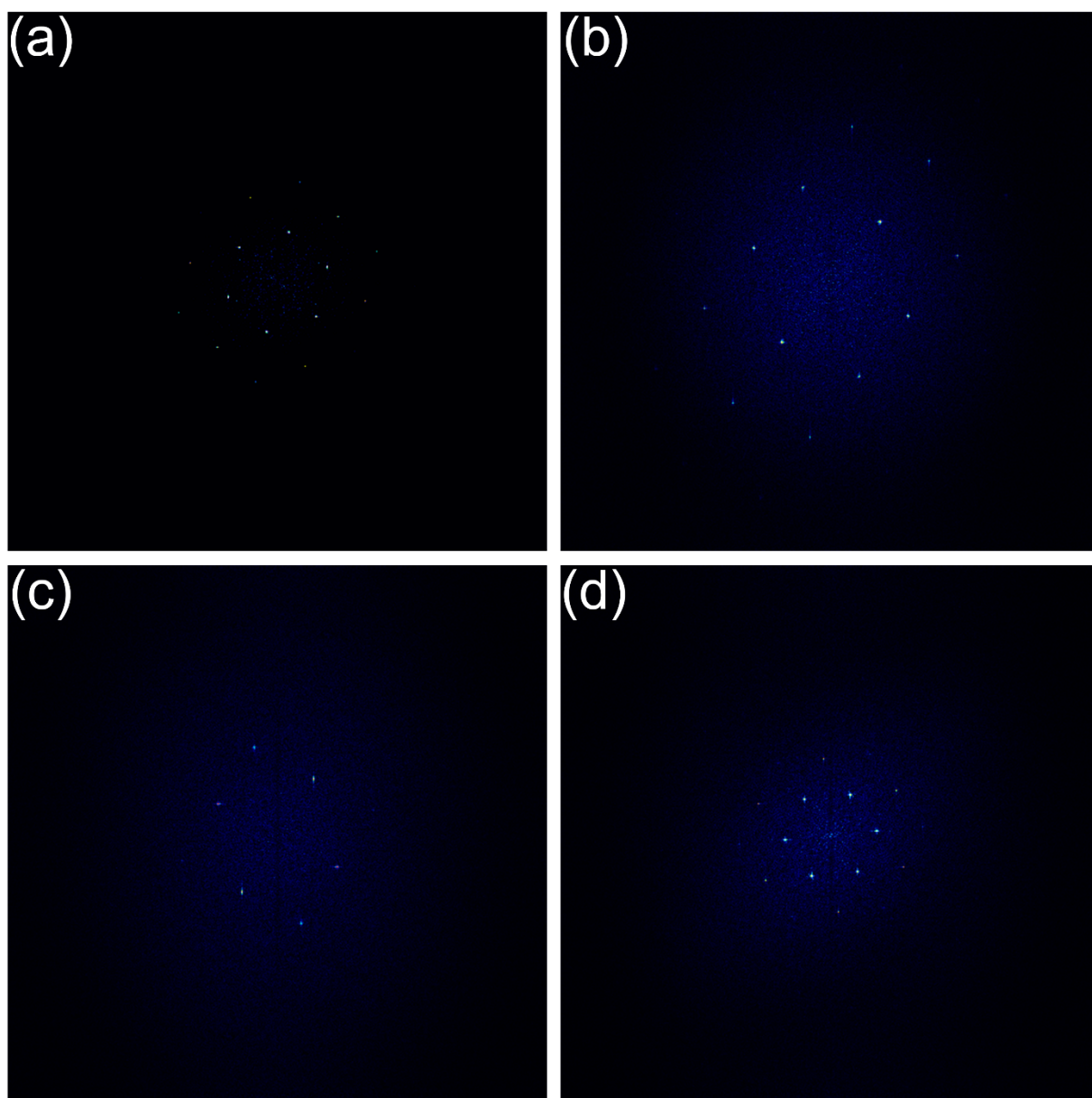


Figure S7. Original 2D-FFT images of the insets in Figs 4b (a), 4c (b), 4d (c), and Fig 7d in the main text.

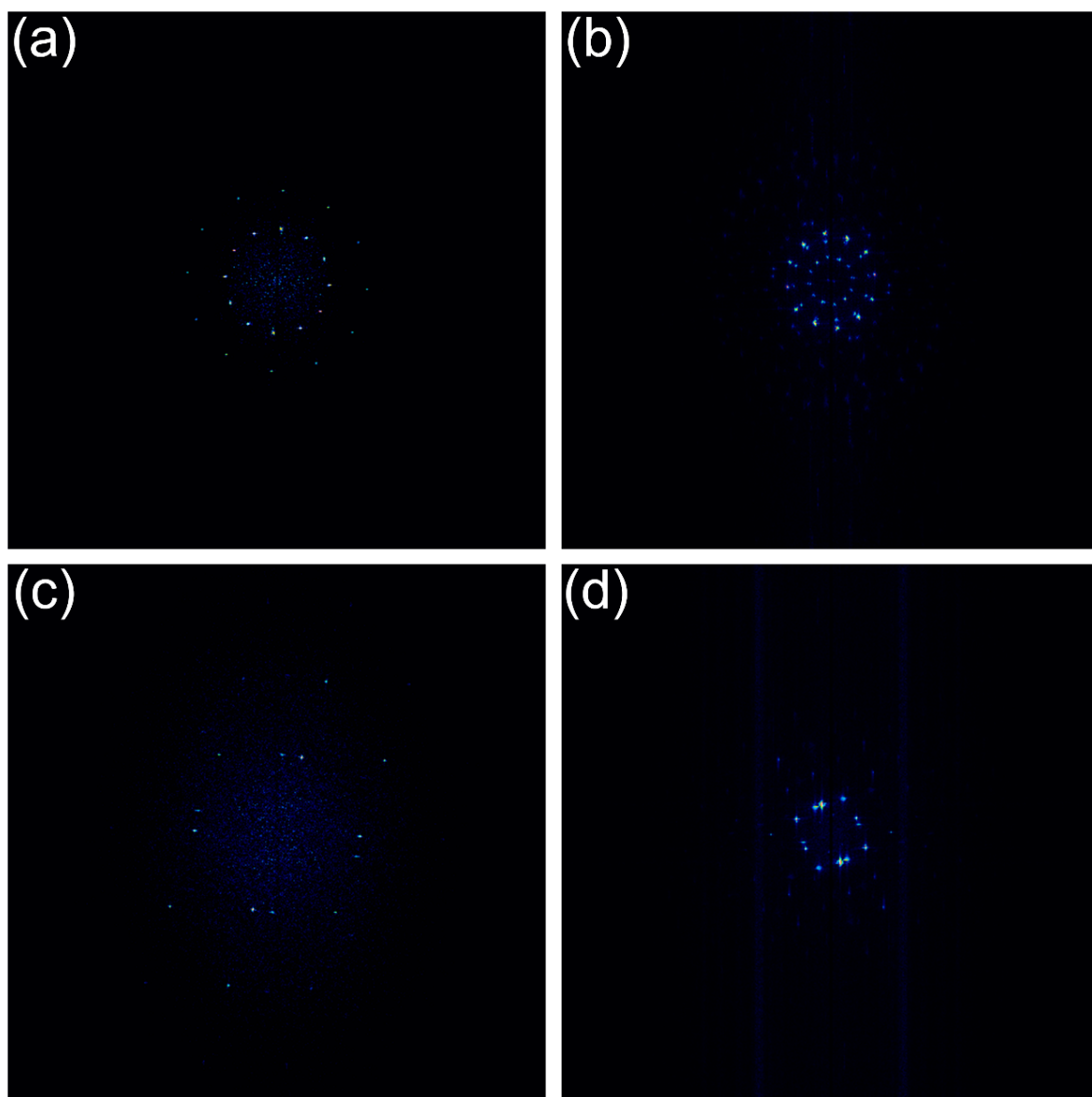


Figure S8. Original 2D-FFT images of Figs 6a (a), 6b (b), 6d (c), and 6e (d) in the main text.

5. Fidelity Analysis

For the fidelity analysis, an in-house program written in Python (ver. 3.6) was used. To minimize the thermal drift effect in the large area STM images ($200\text{ nm} \times 200\text{ nm}$ before calibration), the lateral calibrations were applied to fit the unit cell parameters of respective SAMNs. The coordinates of the bright features (grafted aryl groups) were determined from these calibrated STM images using the Particle & Pore Analysis module of SPIPTM software (ver. 6.0.14 or 6.0.13), in which the origin of the coordinates is an image center. In the detections of the bright features, the features of the apparent height over 100 pm in which detect max particle in 10 pm increment. The further details of the fidelity analysis were reported previously.¹

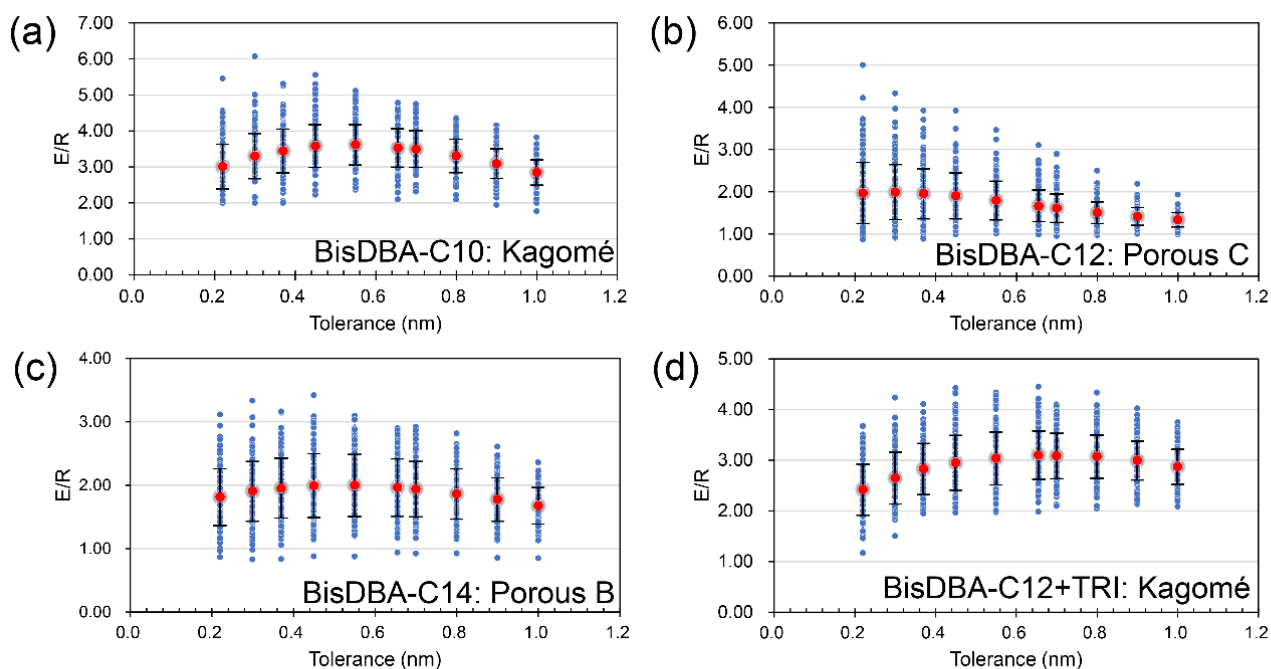


Figure S9. The E/R values at the various tolerances (nm) of the Kagomé (a), Porous C (b), Porous B (c), and Kagomé (d) structures formed by **bisDBA-C10**, **-C12**, and **-C14**, and **bisDBA-C12+TRI**, respectively. Blue dots are the original E/R values of each image. Red dots are the mean E/R values at each tolerance value. Error bars are the standard deviations.

Table S1. The resulted E/R values at different tolerances for the Kagomé, Porous C, Porous B, and Kagomé structures formed by **bisDBA-C10**, **-C12**, **-C14**, and **bisDBA-C12+TRI**, respectively.

template	accepted tolerance (nm)									
	0.22	0.30	0.37	0.45	0.55	0.655	0.70	0.80	0.90	1.00
bisDBA-C10 Kagomé (27) ^a	3.01 ± 0.62	3.30 ± 0.62	3.44 ± 0.61	3.58 ± 0.60	3.62 ± 0.56	3.52 ± 0.54	3.49 ± 0.51	3.31 ± 0.46	3.09 ± 0.41	2.84 ± 0.35
bisDBA-C12 Porous C (30) ^a	1.97 ± 0.72	2.00 ± 0.65	1.95 ± 0.59	1.91 ± 0.54	1.80 ± 0.46	1.66 ± 0.37	1.61 ± 0.34	1.51 ± 0.26	1.42 ± 0.21	1.34 ± 0.17
bisDBA-C14 Porous B (33) ^a	1.81 ± 0.45	1.90 ± 0.47	1.95 ± 0.47	1.99 ± 0.51	1.99 ± 0.49	1.96 ± 0.45	1.94 ± 0.44	1.86 ± 0.40	1.77 ± 0.34	1.67 ± 0.29
bisDBA-C12+TRI Kagomé (34) ^a	2.42 ± 0.50	2.64 ± 0.51	2.82 ± 0.51	2.95 ± 0.54	3.04 ± 0.52	3.10 ± 0.48	3.08 ± 0.45	3.07 ± 0.43	2.99 ± 0.38	2.87 ± 0.35

^aThe numbers of the STM images used for analysis are in parentheses.

6. Additional Fidelity Analysis

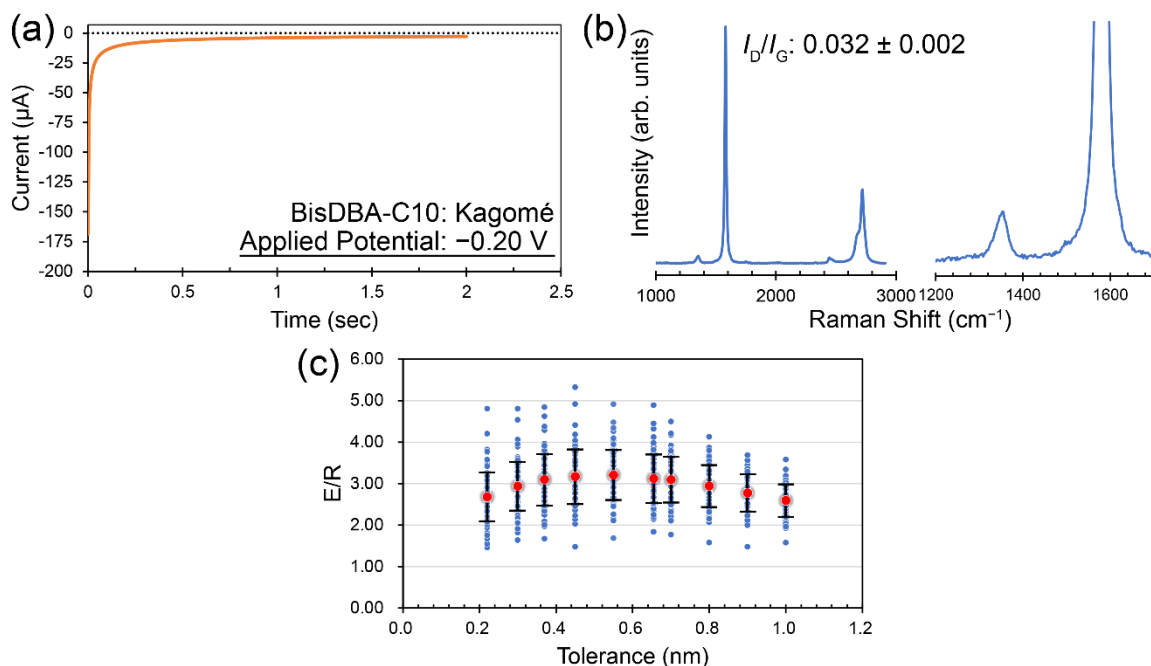


Figure S10. (a, b) Chronoamperogram during the electrochemical grafting of graphite and Raman spectra of the functionalized graphite surface in the presence of a solution of **bisDBA-C10**. The concentration of 3,4,5-trimethoxyaniline was set to be high (1.0 mM). (a) Applied potential for 2 sec. was -0.20 V (vs. Ag/AgCl). (b) Black number in the image is a mean I_D/I_G value. (c) The E/R values at the different tolerances (nm). Blue dots are the original E/R values of each image. Red dots are the mean E/R values at each tolerance value. Error bars are the standard deviations.

We also conducted covalent functionalization of graphite in the presence of **bisDBA-C10** using a solution of 3,4,5-trimethoxyaniline at a higher concentration of 1.0 mM. D peak was observed in Raman spectrum of the functionalized surface. A mean I_D/I_G value was 0.032 ± 0.002 (Figure S10b), which indicates a higher grafting density compared to that (0.021 ± 0.001) using a solution of a lower concentration (0.5 mM; Table 1). In addition, a mean E/R value from the fidelity analysis becomes low.

7. Additional STM Image of Functionalized Surface with bisDBA-C14 Template

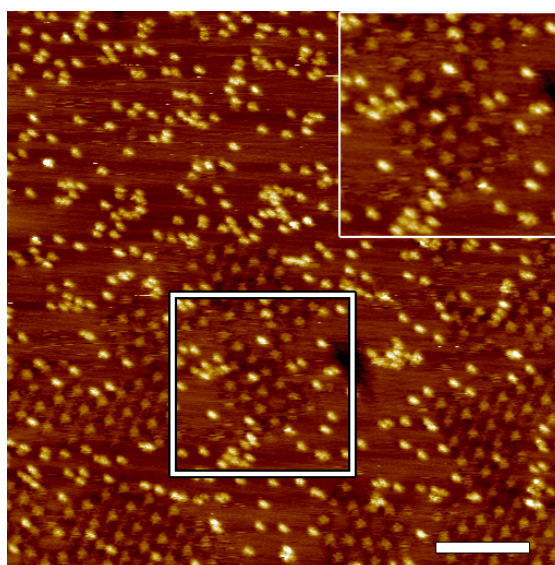


Figure S11. Small area STM image of the functionalized graphite surface using **bisDBA-C14** as the template molecule. Scale bars: 15 nm. Inset: digitally zoomed image of the area highlighted by a white box.

8. Molecular Mechanics (MM) Simulations

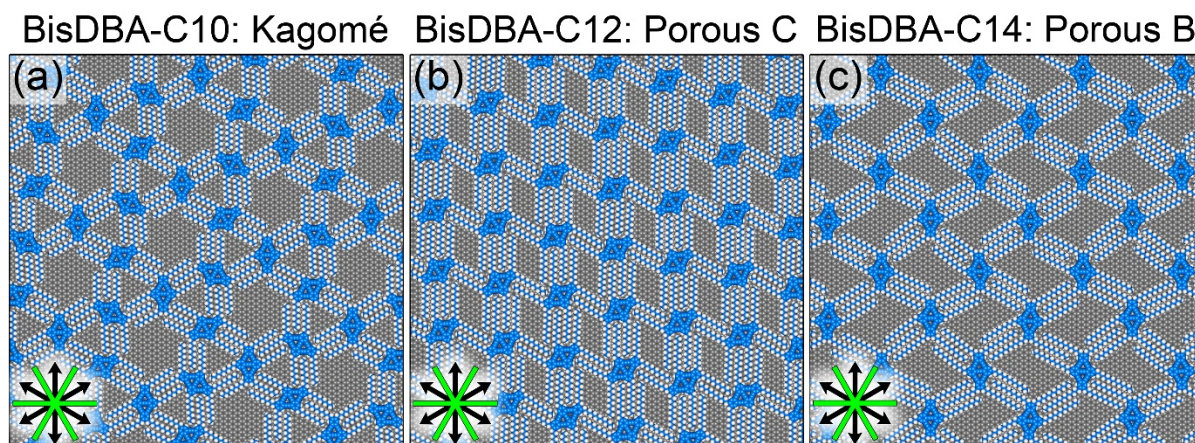


Figure S12. MM optimized (Force field: COMPASS) networks on bilayer graphene sheets under periodic boundary conditions (PBCs; Table S2) of the Kagomé (a), Porous C (b), and Porous B (c) structures formed by **bisDBA-C10**, **-C12** and **-C14**, respectively. Carbon atoms (graphene and **bisDBAs**): grey and blue; hydrogen: white. Black arrows and green lines in the lower left corner indicate the main symmetry axes of the graphene substrate underneath and the in-plane directions normal to those, respectively.

Table S2. PBCs used for the MM simulations.

System	bisDBA-C10 Kagomé	bisDBA-C12 Porous C	bisDBA-C14 Porous B
PBCs	$a = b = 49.923 \text{ nm}$ $\gamma = 60^\circ$	$a = 82.751 \text{ nm}$ $b = 53.378 \text{ nm}$ $\gamma = 75.972^\circ$	$a = 89.460 \text{ nm}$ $b = 44.271 \text{ nm}$ $\gamma = 90^\circ$

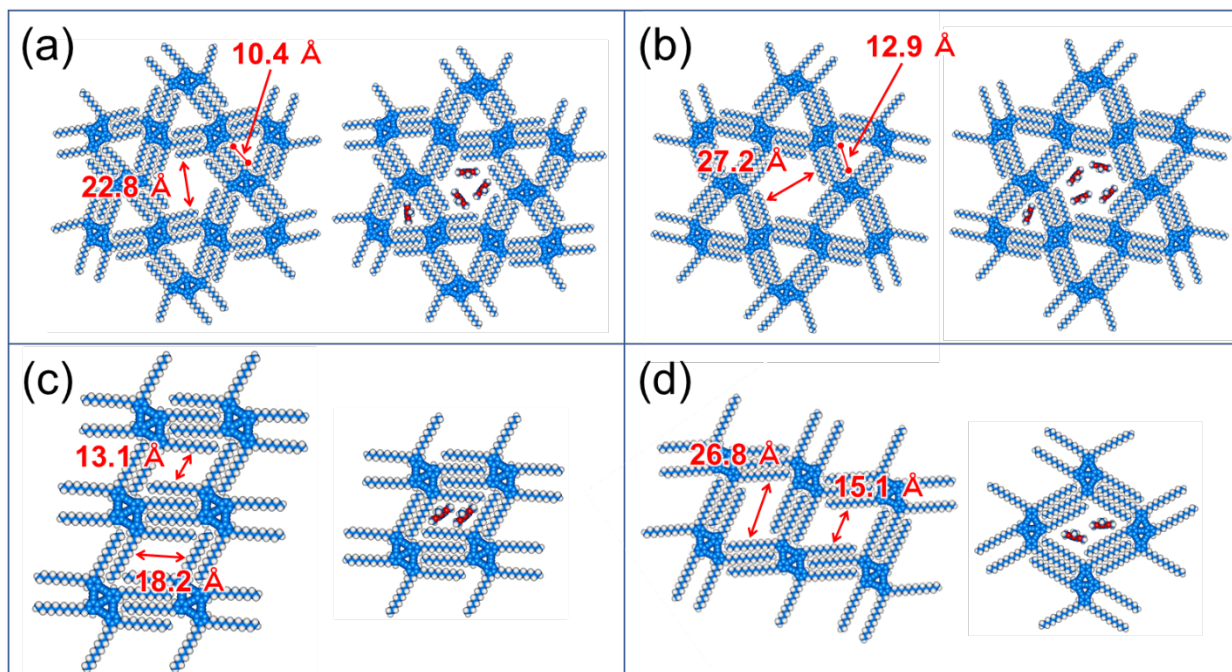


Figure S13. Models of (a, b) the Kagomé structures formed by **bisDBA-C10** and **C12**, respectively, and (c) the Porous C and (d) Porous B structures formed by **bisDBA-C12** and **-C14**, respectively. Left models include the pore size parameters. In the right models, some 1,2,3-trimethoxyphenyl units are placed at the pores for the size comparison.

9. Additional Data for Positional Analysis of Grafted Aryls in Pores

In the case of **bisDBA-C12** or **-C14**, other pores, trigonal and hexagonal pores were also observed in addition to the quadratic pore. The distributions of those pores are summarized in Table S3.

Table S3. Statistical analysis of the distribution of the trigonal, quadrangular, pentagonal, and hexagonal pores formed by **bisDBA-C12** and **-C14** after the covalent functionalization.

template molecule	pore shape			
	Trigonal pore ^a	Quadrangular pore	Pentagonal pore	Hexagonal pore ^a
bisDBA-C12	5.4%	92.6%	<0.1%	1.9%
bisDBA-C14	2.4%	96.1%	0%	1.5%

^a The trigonal and hexagonal pores are attributed to the small domains of the Kagomé structure, which has never been observed before the covalent functionalization.

In addition to the tetragonal pore, we also analyzed the number of the bright features observed in the Kagomé structures formed by **bisDBA-C12** and **-C14** on the functionalized surface (Table S4).

Table S4. Summary of the distribution of the number of bright features in the hexagonal or trigonal pores of the Kagomé structures formed by **bisDBA-C12** and **bisDBA-C14** on the functionalized surfaces.

template molecule	number of bright features in hexagonal pore		number of bright features in trigonal pore	
	0	1	0	1
bisDBA-C12 Kagomé	28.6%	71.4%	91.7%	8.3%
bisDBA-C14 Kagomé	42.9%	57.1%	100%	0.0%

10. Covalent Functionalization around the Domain Boundary

In the case of **bisDBA-C14**, we only observed the orientational domains of the porous B structure because of a C_3 symmetric graphite lattice. The smallest angle of the orientational domains is only 60° , which was confirmed by a few STM images at the domain boundary (Figure S14). Thus, it is orientationally achiral. Moreover, the relative orientations of the alignment of the grafted aryl units were also 60° .

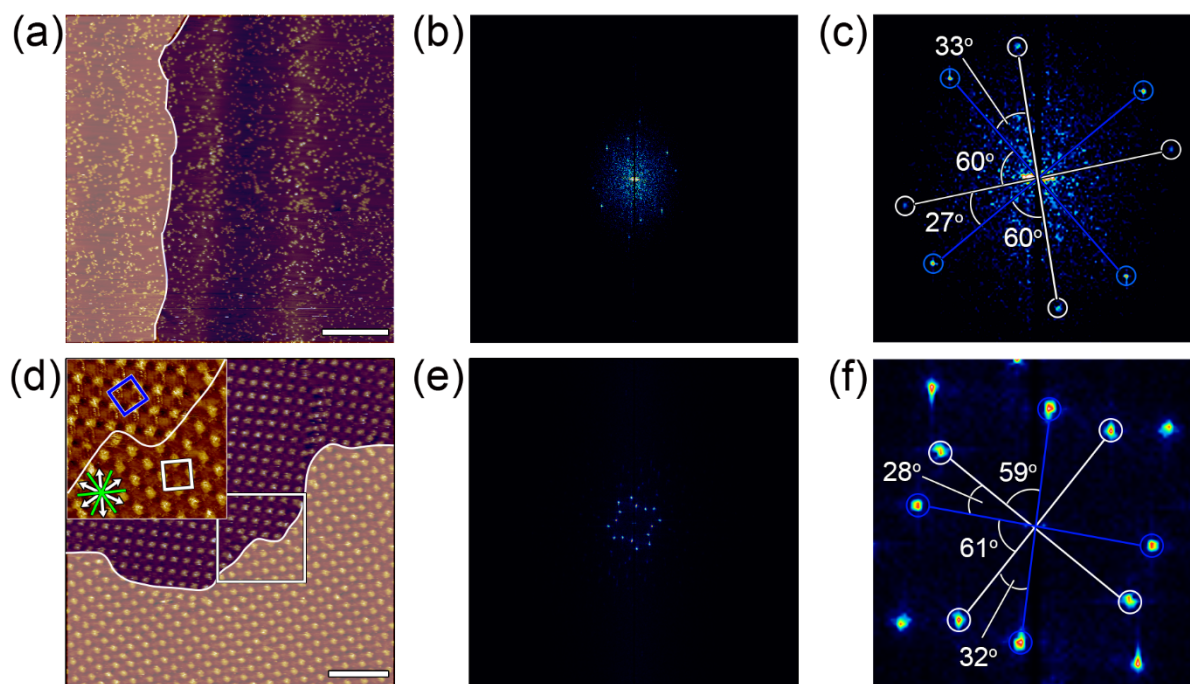


Figure S14. (a) Large area STM image of the functionalized graphite surface in the presence of a solution of **bisDBA-C14** in TCB as the interfacial layer. Covalent functionalization was conducted using CA. The concentration of 3,4,5-trimethoxyaniline was set to be 0.5 mM. (b) 2D-FFT image of image (a), and (c) a digitally zoomed image of image (b). (d) Large area STM image of the Porous B structure formed by **bisDBA-C14**. Inset is high-resolution STM image at the area surrounded by a white square, showing two chiral structures divided by the domain boundary (white line). Blue and white rhombi are unit cells of these structures. White arrows and green lines indicate the main symmetry axes of the graphite substrate underneath and the in-plane directions normal to those, respectively. (e) 2D-FFT image of the image (d), and (f) a digitally zoomed image of image (e). (a, d) White lines are domain boundaries. Scale bars: (a) 40 nm; (d) 15 nm. Tunneling parameters: (a) $V_{\text{bias}} = -0.60$ V, $I_{\text{set}} = 80$ pA; (d) $V_{\text{bias}} = -1.14$ V, $I_{\text{set}} = 117$ pA; (inset of d) $V_{\text{bias}} = -1.06$ V, $I_{\text{set}} = 124$ pA. (c, f) In 2D-FFT images, two sets of rectangular periodicities were detected. The angles between the lines connecting signals and the center of images are identical between the functionalized surface and original SAMN templates.

11. Additional STM Images of SAMN Formed by BisDBA-C12

11-1. Control Experiment of STM Observation of SAMN Formed by BisDBA-C12

We performed a control experiment of STM observation using a solution of **bisDBA-C12** in TCB whose concentration was set to be identical to that of a solution of **bisDBA-C12+TRI** in TCB (9.9×10^{-7} M). The STM observation was performed at room temperature after annealing at 80 °C for 2 h. Exclusive formation of a Porous C structure was observed (Figure S15).

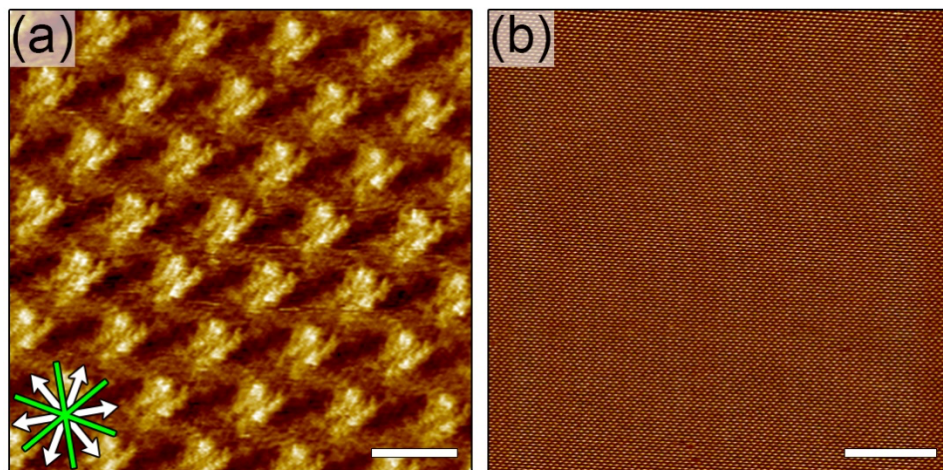


Figure S15. (a) High resolution and (b) large area STM images of SAMN formed by **bisDBA-C12** at the TCB/graphite interface at room temperature after annealing at 80 °C for 2 h. The concentration of **bisDBA-C12** was 9.9×10^{-7} M. White arrows in the lower left corner and green lines indicate the main symmetry axes of graphite substrate underneath and the in-plane directions normal to those, respectively. Scale bars: (a) 3 nm; (b) 40 nm. Tunneling parameters: $V_{\text{bias}} = -1.14$ V, $I_{\text{set}} = 304$ pA.

11-2. 2D Chirality of Kagomé Structure Formed by BisDBA-C12+TRI

In the STM observations of SAMNs of **bisDBA-C12+TRI**, there are two enantiomorph domains (CW or CCW) of the Kagomé structure similar to **bisDBA-C10** (Figure S16). Angle α is $\pm 16 \pm 1^\circ$ (+ and – signs for the CW and CCW structures).

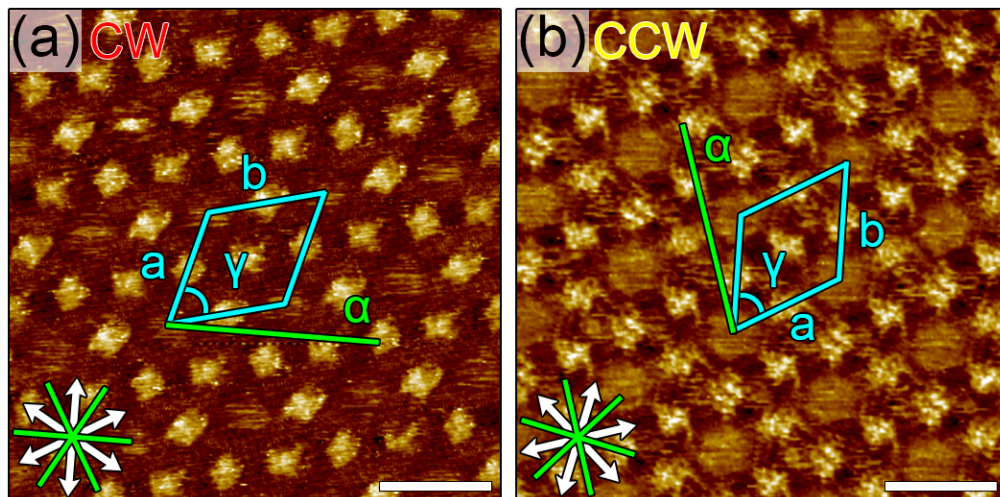


Figure S16. High-resolution STM images of the CW (a) and CCW (b) structures of the Kagomé structure formed by **bisDBA-C12+TRI**. White arrows in the lower left corner and green lines indicate the main symmetry axis of graphite substrate underneath and the in-plane directions normal to those, respectively. Turquoise rhombi in the images are unit cells. Unit cell parameter and angle α are summarized in Table 1 in the main text. Scale bars: 5 nm. Tunneling parameters: (a) $V_{\text{bias}} = -0.78$ V, $I_{\text{set}} = 1767$ pA; (b) $V_{\text{bias}} = -0.90$ V, $I_{\text{set}} = 194$ pA.

11-3. Chirality Transfer from the Kagomé Structure Formed by BisDBA-C12 + TRI

In the template-guiding covalent functionalization using the Kagomé structure formed by **bisDBA-C12+TRI**, chirality transfer was also confirmed (Figure S17).

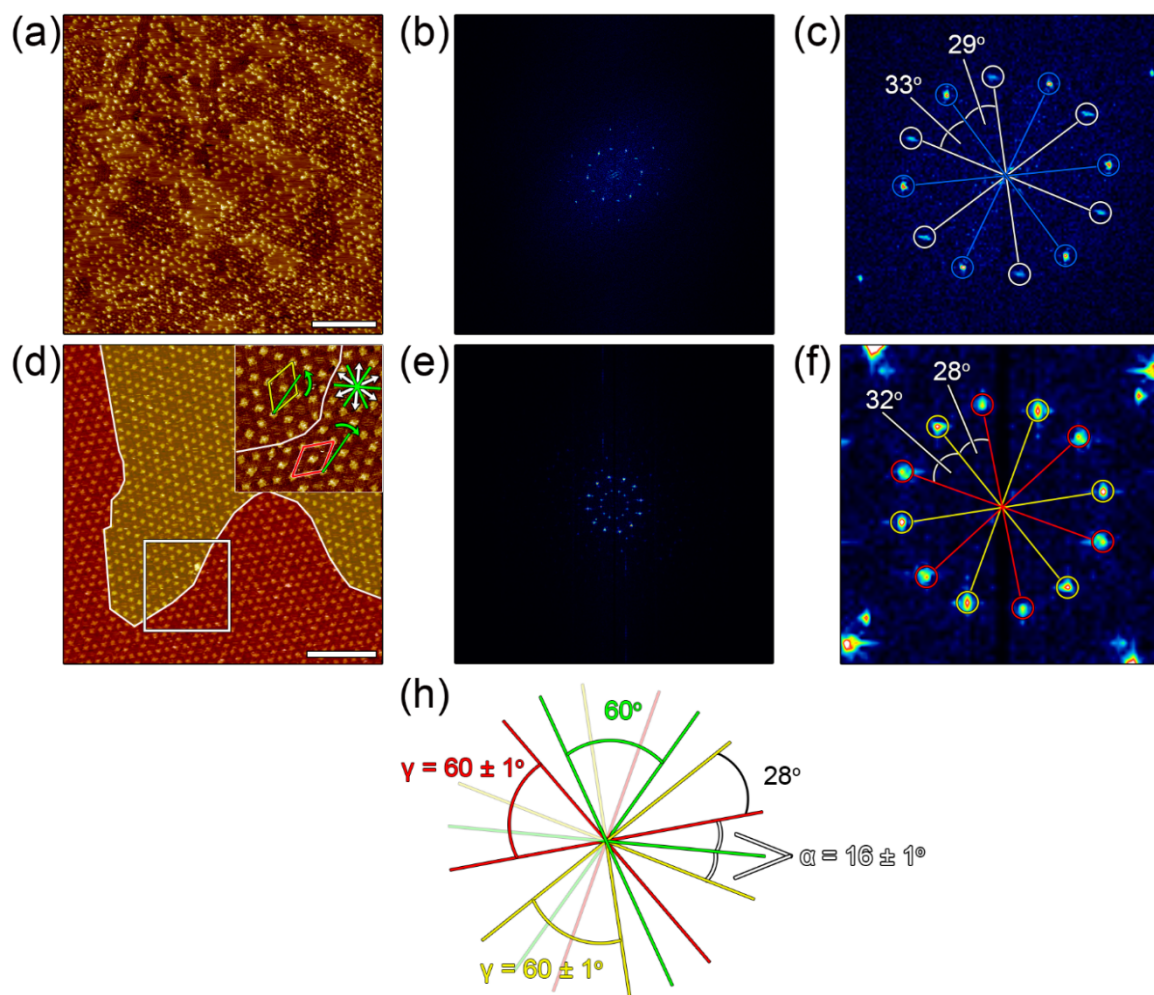


Figure S17. (a) Large area STM images of the functionalized graphite surfaces in the presence of a solution of **bisDBA-C12+TRI** in TCB as an interfacial layer. Covalent functionalization was conducted using CA. The concentration of TMeOD was set to be 0.5 mM. (b) 2D-FFT images of (a), and (c) digitally zoomed image of (b). (d) Large area STM images of a Porous B structure formed by **bisDBA-C12+TRI**. Inset is a high-resolution STM image of a white square area, showing the two enantiomeric structures with domain boundaries. Yellow and red rhombi are unit cells of these structures. White arrows and green lines indicate the main symmetry axes of the graphite substrate underneath and the in-plane directions normal to those, respectively. (e) 2D-FFT images of image (d), and (f) a digitally zoomed image of (e). (a, d) White lines are domain boundaries. Scale bars: (a) 40 nm; (d) 20 nm. Tunneling parameters: (a) $V_{\text{bias}} = -0.50$ V, $I_{\text{set}} = 80$ pA; (d and its inset) $V_{\text{bias}} = -0.78$ V, $I_{\text{set}} = 176$ pA. (c, f) In 2D-FFT images, two sets of hexagonal periodicities were detected. The angles between the lines connecting signals and the center of images are identical between the functionalized surface and SAMNs (28° and 32°) (h) Schematic model for the relationship of the angles between two chiral unit cell vectors and the normals to the graphite main symmetry axes. Red, yellow and green lines represent unit cell vectors of the CW structure, that of the CCW structure, and the normals to the graphite main symmetry axes, respectively.

12. Reference

- 1 K. Tahara, Y. Kubo, S. Hashimoto, T. Ishikawa, H. Kaneko, A. Brown, B. E. Hirsch, S. De Feyter and Y. Tobe, *J. Am. Chem. Soc.*, **2020**, *142*, 7699–7708.